Published in final edited form as:

J Cell Biochem. 2018 March ; 119(3): 2636–2645. doi:10.1002/jcb.26429.

Mesoderm specific transcript localization in the ER and ER-lipid droplet interface supports a role in adipocyte hypertrophy

Igor Prudovsky[1,2], **Rea P. Anunciado-Koza**[1], **Chester G. Jacobs**[1], **Doreen Kacer**[1], **Matthew E. Siviski**[1,2], and **Robert A. Koza**[1,2,*]

[1]Center for Molecular Medicine, Maine Medical Center Research Institute, Scarborough, Maine 04074

[2]The Graduate School of Biomedical Science and Engineering, University of Maine, Orono, Maine 04469

Abstract

Highly variable expression of mesoderm specific transcript (*Mest*) in adipose tissue among genetically homogeneous mice fed an obesogenic diet, and its positive association with fat mass expansion, suggests that *Mest* is an epigenetic determinant for the development of obesity. Although the mechanisms by which MEST augments fat accumulation in adipocytes have not been elucidated, it has sequence homology and catalytic peptide motifs which suggests that it functions as an epoxide hydrolase or as a glycerol- or acylglycerol-3-phosphate acyltransferase. To better understand MEST function, detailed studies were performed to precisely define the intracellular organelle localization of MEST using immunofluorescence confocal microscopy. Lentiviral-mediated expression of a C-terminus Myc-DDK-tagged MEST fusion protein expressed in 3T3-L1 preadipocytes/adipocytes, and ear-derived mesenchymal stem cells (EMSC) from mice was observed in the endoplasmic reticulum (ER) membranes and is consistent with previous studies showing endogenous MEST in the membrane fraction of adipose tissue. MEST was not associated with the Golgi apparatus or mitochondria; however, frequent contacts were observed between MEST-positive ER and mitochondria. MEST-positive domains were also shown on the plasma membrane (PM) of non-permeabilized cells but they did not co-localize with ER-PM bridges. Post-adipogenic differentiated 3T3-L1adipocytes and EMSC showed significant co-localization of MEST with the lipid droplet surface marker perilipin at contact points between the ER and lipid droplet. Identification of MEST as an ER-specific protein that co-localizes with lipid droplets in cells undergoing adipogenic differentiation supports a function for MEST in the facilitation of lipid accumulation and storage in adipocytes.

Keywords

MESODERM SPECIFIC TRANSCRIPT; ENDOPLASMIC RETICULUM; ADIPOCYTE; ADIPOGENESIS; LIPOGENESIS; LIPID DROPLET

*Correspondence to: Robert A. Koza, Ph.D., Maine Medical Center Research Institute, 81 Research Drive, Scarborough, ME 04074, rkoza@mmc.org.

INTRODUCTION

Mesoderm specific transcript (*Mest*), an imprinted gene predominantly expressed from the paternal allele, has been shown to be rapidly and highly induced in adipose tissue in mice fed an obesogenic diet and its expression is positively associated with inter-individual variation of adipose tissue expansion (ATE) in inbred mice (Koza, Nikonova et al. 2006, Nikonova, Koza et al. 2008). The highly variable expression of *Mest* and positive association with adipose tissue expansion within isogenic murine populations presents a model for an epigenetic component in the regulation of ATE. Studies using *in vitro* and *in vivo* transgenic models that overexpress *Mest* support its role in promoting adipocyte hypertrophy (Takahashi, Kamei et al. 2005), whereas mice with global and adipose tissue preferential inactivation of *Mest* showed reduced adiposity and improved glucose tolerance when fed a HFD (Anunciado-Koza, Manuel et al. 2017). Our studies and those of others suggest that strategies that inhibit MEST function in adipocytes could lead to reduced adipocyte hypertrophy and attenuation of adipose tissue inflammation and dysregulation of glucose homeostasis (Meijer, de Vries et al. 2011, Sanjabi, Dashty et al. 2015).

MEST belongs to a family of α/β-hydrolase proteins that have a variety of catalytic activities (Ollis, Cheah et al. 1992, Holmquist 2000); however, its role has not been defined. A conserved epoxide-coordinating tyrosine in its sequence and homology with epoxide hydrolases from *M. tuberculosis* suggests that MEST could as an epoxide hydrolase (Kaneko-Ishino, Kuroiwa et al. 1995, Decker, Arand et al. 2009) to modulate epoxy- and diol-fatty acid derivatives, which are thought to be endogenous mediators of PPARs (Cowart, Wei et al. 2002, Fang, Hu et al. 2005, Fang, Hu et al. 2006, Spector and Norris 2007, Spector 2009, Kim, Vanella et al. 2010, Zha, Edin et al. 2014, Waldman, Bellner et al. 2016). In addition, MEST also contains the catalytic triad serine-histidine-aspartate (amino acids 145–147), which is associated with the function of serine proteases, lipases and acyltransferases, further suggesting a role in triglyceride metabolism and lipid storage (Carter and Wells 1988, Holmquist 2000). Western blot analysis of subcellular fractions of adipose tissue shows MEST to be enriched in fractions that contain the ER protein calnexin but could not distinguish whether MEST is also localized within the Golgi complex or lipid droplet membrane (Nikonova, Koza et al. 2008). Unfortunately, since the rabbit polyclonal antibodies for MEST used in the subcellular fractionation studies are not suitable for immunofluorescence microscopy, alternative strategies must be used for detailed analyses of MEST localization within cells. A recent study that cursorily assessed HEK293 cells transfected with plasmids expressing Myc-tagged MEST and enhanced cyan fluorescent protein (ECFP), a soluble protein that localizes to the lumen of the ER, supports the tissue fractionation results and shows modest co-localization between MEST and ECFP in the ER (Jung, Lee et al. 2011). However, to precisely evaluate the subcellular localization of MEST with respect to lipid droplet formation, we generated stable clones of adipogenic 3T3-L1 preadipocytes and primary mesenchymal progenitor cells that express a C-terminal Myc-DDK tagged MEST fusion protein. The studies herein support a subcellular location of MEST that is consistent with a potential role in facilitating adipose tissue expansion.

METHODOLOGY

GENERATION OF STABLE CELL LINES EXPRESSING MEST

3T3-L1 preadipocytes purchased from Zen-Bio were cultured in growth medium composed of DMEM (Corning), 10% iron-supplemented bovine calf serum (Hyclone) and Normocin (100 μg/ml, InvivoGen). Sub-confluent pre-adipocytes were transduced with lentiviral particles based on the pLenti-EF1a-C-Myc-DDK-IRES-Puro vector (Origene, PS100085) containing the *Mest* cDNA sequence. Viral particles were packaged at the Maine Medical Center Research Institute Cell Culture and Viral Vector Core. Stable clones expressing *Mest* were selected using growth medium supplemented with selective agent puromycin (1 μg/ml, Sigma). Ear mesenchymal stem cells (EMSCs) were isolated as previously described (Rim, Mynatt et al. 2005, Gawronska-Kozak 2014) from wildtype mice (+/+) and mice with a homozygous inactivation of *Mest* (KO/KO). Cells were cultured in 5% CO_2 and maintained in DMEM/F-12 (Life Technologies) supplemented with 15% heat inactivated FBS (Life Technologies), Primocin (100 μg/ml, InvivoGen) and recombinant murine basic FGF (10 ng/ml, Peprotech). EMSCs were transduced with lentiviral vector (Origene, PS100085) as described above and stable clones expressing *Mest* were established using growth medium with 4 μg/ml puromycin.

DNA TRANSFECTION

Transfection of MAPPER-GFP plasmid (Chang, Hsieh et al. 2013, Dickson, Jensen et al. 2016) into undifferentiated stable 3T3-L1 cells overexpressing *Mest* with C-terminal Myc-DDK tag was performed using the Nucleofector 2b system (Lonza) and the Amaxa Cell Line Nucleofector Kit V. Cells were harvested and resuspended in Nucleofector solution at 1×10^6 cells/100 μl. MAPPER-GFP plasmid (2 μg) was added to the cells and transfection was performed using Nucleofector Program T-030. The cells were then plated in 6-well plates with fibronectin-coated coverslips for confocal microscopy. After overnight incubation, cells were rinsed gently in in 1X PBS and fixed in 10% neutral buffered formalin.

ADIPOGENIC STIMULATION

Subconfluent 3T3-L1 cultures were trypsinized (0.05% trypsin-EDTA, Life Technologies) and seeded at 50,000 cells/well in 6 well plates with fibronectin-coated coverslips. Adipogenesis was induced in cells 48 hrs after achievement of full confluence using adipogenic medium I consisting of DMEM, FBS (10%, Sigma), 1X Pen-Strep, 3-Isobutyl-1-methylxanthine (0.5 mM IBMX, Sigma), dexamethasone (1 μM, Sigma) and, recombinant human insulin (1.7 μM, Sigma) for 48 hours. This was followed with adipogenic medium II composed of DMEM, 10% FBS, 1X Pen-Strep and 0.425 μM insulin for another 48 hrs. Cells were then maintained in DMEM, 10% FBS and 1X Pen-Strep until harvest. Cells were washed in 1X PBS and fixed in 10% neutral buffered formalin. EMSCs were seeded at 100,000 cells/well in 6 well plates. To induce adipocyte differentiation, confluent EMSCs were cultured for 48 hrs in DMEM/F-12 supplemented with 5% heat inactivated FBS, Primocin, 1.7 μM insulin, 0.5 mM 3-Isobutyl-1-methylxanthine and 1 μM dexamethasone. On day 2 and every 2–3 days thereafter, cells were cultured in DMEM/F-12 supplemented

with 5% heat inactivated FBS, Primocin, 17 nM insulin and 2 μM rosiglitazone (Sigma). Differentiation of cells was assessed by microscopic evaluation of lipid droplet formation.

QUANTITATIVE REVERSE TRANSCRIPTION PCR

Total RNA was isolated from cells using TriReagent (Molecular Research Center) as described (Nikonova, Koza et al. 2008). Quantitative reverse transcription-PCR was performed using total RNA with specific primers and probes designed using Primer Express software v3.0.1 (Life Technologies). TaqMan probes (Biosearch Technologies) were used for gene quantification using TaqMan® RNA-to-CT 1-Step Kit (Life Technologies). Gene expression data are presented as arbitrary units (AU) normalized to either TATA box binding protein (*Tbp*) or total nanograms (ng) of input RNA/reaction. RNA input was quantified using Qubit HS RNA Assay Kit (Life Technologies). Quantitative PCR was performed using the CFX384 Real Time PCR detection system (BioRad).

WESTERN BLOT ANALYSIS

Total cellular protein was collected in RIPA buffer (50 mM Tris pH 7.4, 150 mM NaCl, 1 mM EDTA, 0.1% SDS, 1% IGEPAL® CA-630, 0.25% sodium deoxycholate) supplemented with protease and phosphatase inhibitor cocktails (Sigma). Protein was quantified using the Pierce™ protein assay kit (ThermoFisher Scientific). Subcellular fractionation in undifferentiated and differentiated cells was performed as described (Harris, Shew et al. 2012). Briefly, cells grown in at least 3 × 10 cm dishes were pooled. Cells were washed with ice-cold PBS, scraped in a small volume of PBS and transferred to a 2 ml tube. Cells were pelleted by centrifugation and the supernatant discarded. The pellet was resuspended in 60% sucrose dissolved in lysis buffer pH 7.4 (10 mM HEPES, 1 mM EDTA). Lysis buffer (~800 μl) was added to the suspension and cells were disrupted by passing 5X through a 27-gauge blunt-tip needle. A mix of 2 μl 0.05% brilliant blue FCF dye (ThermoFisher Scientific) per 1 ml lysis buffer was prepared and 600 μl was overlaid on top of the cell homogenate. The homogenate was centrifuged for 2 hrs at 20,000 × g at 4°C. The entire tube was frozen at −70°C to facilitate a clean cut. Floating, soluble and membrane fractions were collected and protein content quantified as described earlier.

Western blotting was performed with the Mini-Protean Tetra Cell and Mini Trans-Blot Electrophoretic Transfer cell (Bio-Rad). Nitrocellulose blots (GE Healthcare) were incubated with antibodies against MEST (rabbit polyclonal generated in our laboratory, 1:5000), DDK (FLAG) (OriGene mouse monoclonal, 1:20,000), perilipin (Cell Signaling rabbit monoclonal, 1:10,000), PDI (Cell Signaling rabbit monoclonal, 1:10,000), GAPDH (Cell Signaling rabbit monoclonal, 1:10,000) and calreticulin (Cell Signaling rabbit monoclonal, 1:10,000). Membranes were blocked overnight in 1% fish gelatin (Amresco) in PBS-T (0.1%) or 10% non-fat dry milk in PBS. Membranes were incubated overnight at 4°C in the primary antibody and then secondary antibody at RT for 1 hour. Antibodies were diluted in either the blocking buffer or Signal Boost Immunoreaction Enhancer (EMD Millipore). Signals were detected by chemiluminescence (WesternSure Premium Chemiluminescent Substrate, Li-Cor). Blots were exposed to X-ray Film and/or imaged using the C-Digit Blot Scanner (Licor). Stripping of blots was performed using Re-blot Plus Stripping Solution (EMD Millipore) per manufacturer's instructions.

CONFOCAL IMMUNOFLUORESCENCE MICROSCOPY

3T3-L1 cells and EMSC stably transfected with MEST-Myc-DDK were fixed with 4% neutral formaldehyde, washed with PBS and incubated for 30 min in blocking buffer (BB; PBS with 5% bovine serum albumin, 0.1% Tween 20 and 0.1% sodium azide). In all studies, to detect MEST-Myc-DDK, cells were incubated for 1 h with a 1:500 dilution of CY3-conjugated mouse monoclonal anti-Myc antibodies (Sigma) in BB. Nuclei were stained with 0.1 μg/ml Hoechst 33258 (Sigma) in BB and filamentous actin was stained with Alexa-488 conjugated phalloidin (Invitrogen). Co-localization of MEST with endoplasmic reticulum, lipid droplets and mitochondria was studied using 1 h incubation with a 1:500 dilution of rabbit monoclonal antibodies against PDI (Cell Signaling), perilipin (Cell Signaling) or mitochondrial hexokinase (Cell Signaling), followed by a PBS wash and 30 min incubation with BB containing Cy3-conjugated anti-Myc antibodies, Hoechst, and a 1:500 dilution of Alexa 488-conjugated goat anti-rabbit IgG antibodies (Invitrogen). To co-localize MEST and Golgi apparatus, cells were incubated for 1h in BB with a 1:500 dilution of mouse monoclonal antibodies to GM130 (BD Biosciences) and then for 30 min with Alexa 488 conjugated goat antibodies against mouse IgG (Invitrogen). Then, cells were blocked for 1h in BB containing 1 mg/ml mouse IgG (Sigma) and after that incubated for 30 min with CY3-conjugated mouse monoclonal anti-Myc antibodies and Hoechst. Cells were studied using a Leica SP8 confocal microscope at the Maine Medical Center Research Institute Confocal Microscopy Facility. Negative controls using secondary antibodies only were completely devoid of fluorescent signal (not presented). Deconvolution of 3D stacks and reconstruction of 3D images was achieved using the Imaris program on a dedicated computer.

RESULTS

RETICULAR PATTERN OF MEST DISTRIBUTION IN CYTOPLASM

Tissue and cell fractions enriched for cellular components analyzed by Western blot supports MEST as an ER and/or Golgi body localized protein; however, detailed confocal microscopic studies to visualize MEST's intracellular localization relative to surrounding cellular structures has not been performed. Such studies have been impeded by the lack of appropriate anti-MEST antibodies. Indeed, all available anti-MEST antibodies including those produced in our laboratory are effective for immunoblotting but not for immunofluorescence. This discrepancy could be explained by a potential localization of MEST in the plasma membrane resulting in a cytotoxic effect of immunoglobulins recognizing non-denatured MEST in antibody-producing animals. Conversely antibodies binding denatured MEST, while being biologically inactive, could only recognize MEST resolved using SDS-PAGE and Western blot.

To overcome the issue with MEST antibodies, we have used lentiviral transduction to stably express Myc-DDK-tagged MEST fusion protein in mouse ear-derived mesenchymal stem cells (EMSC) and in 3T3-L1 preadipocytes in both the undifferentiated state and after chemical induction of adipogenesis. Cell lines derived from 3T3-L1 and EMSC with stable expression of Myc-DDK-tagged MEST (MEST-Myc-DDK) show high expression of MEST-Myc-DDK mRNA (Fig. 1A) and protein (Fig. 1B) compared to non-transduced cells or cells

transduced with lentivirus with an empty vector (EV). Furthermore, MEST-Myc-DDK co-localizes with the ER marker calreticulin (CALR) in the membrane fraction of 3T3-L1 preadipocytes and adipocytes before (day 0) and after (day 3) initiation of adipogenic differentiation whereas perilipin (PLIN1), localized within lipid droplet membranes, is only observed in the floating fraction (FF) at day 3 (Fig. 1C). These results faithfully recapitulate previous studies that show MEST localized within the membrane fraction of murine adipose tissue (Nikonova, Koza et al. 2008).

In formalin fixed 3T3-L1 and EMSC cells stained with anti-Myc antibodies, irrespective of their differentiation status, transduced MEST-Myc-DDK exhibited a reticular pattern of distribution in cytoplasm (Fig. 2). Although the interior of nuclei was MEST-negative, the nuclear envelope was strongly MEST-positive (Fig. 2A, B). In addition, patterns of reticular staining were similar between undifferentiated 3T3-L1 preadipocytes (Fig. 2A) and differentiated EMSC adipocytes (Fig. 2B). Interestingly, we did not observe a distinct MEST staining of the plasma membrane shown by minimal co-localization of peripheral filamentous actin and MEST in EMSC derived from wildtype of *Mest* knockout mice (Fig. 2C, D). The reticular pattern and nuclear envelope localization for MEST was similar to that observed in a superficial immunofluorescent microscopic evaluation of the co-localization between plasmid expressed MEST-Myc and ECFP (enhanced cyan fluorescent protein)-ER in HEK-293 cells (Jung, Lee et al. 2011).

MEST IS LOCALIZED IN THE MEMBRANES OF ENDOPLASMIC RETICULUM

Considering the reticulated pattern of MEST distribution in the cytoplasm, we used MEST-Myc-DDK transduced EMSC and 3T3-L1 preadipocytes to explore whether MEST is localized in the endoplasmic reticulum (ER). MEST and ER were detected using anti-Myc antibodies and antibodies against protein disulfide-isomerase (PDI), a specific marker of ER matrix. Both EMSC and 3T3-L1preadipocytes showed strong co-localization of MEST and ER (Fig. 3A, B) that was further confirmed by three-dimensional confocal cell reconstruction (Supplemental Movie 1). Specifically, MEST was localized in ER membranes and this localization was especially obvious in extended cisterns of ER (Supplemental Figure 1).

GOLGI APPARATUS, MITOCHONDRIA AND LIPID DROPLETS ARE MEST-FREE

To study the potential relation of MEST to other membranous organelles, we have used antibodies against the Golgi matrix protein GM130 and mitochondrial enzyme hexokinase. Surprisingly, in spite of well-documented bidirectional vesicular traffic between Golgi and ER (Barlowe 1995, Lewis and Pelham 1996, Watson and Stephens 2005, Spang 2013), the Golgi apparatus in both EMSC and 3T3-L1 cells was devoid of MEST (Fig. 4A, B). These data are especially interesting, considering a high density of membranes in Golgi. Similarly, mitochondria were also found to be MEST-free, however they exhibited frequent contacts with MEST-positive ER (Fig. 4C, D).

Lipid droplets, organelles actively accumulated in the course of adipogenic differentiation for storage of triglycerides, have been suggested to form as a result of local budding of nascent lipid droplets from ER channels which culminates by the detachment of mature

droplets from ER (Guo, Cordes et al. 2009, Fujimoto and Parton 2011, Prinz 2013, Wilfling, Wang et al. 2013, Pol, Gross et al. 2014). To detect lipid droplets, we used the antibodies to the specific lipid droplet surface marker perilipin (Fig. 5A, B). Interestingly, although lipid droplets in both differentiated EMSC and 3T3-L1 adipocytes were mostly devoid of MEST, significant co-localization of perilipin and MEST occurred at contact points between the ER and lipid droplets. This proximity of ER-localized MEST with lipid droplets may indicate a functional role for MEST in lipid droplet formation.

LIMITED MEST-POSITIVE DOMAINS ON THE SURFACE OF PLASMA MEMBRANE

The failure to observe a continuous MEST positivity of plasma membrane prompted us to change the conditions of cell staining by omitting Triton X100 from the blocking buffer that would allow the exclusive detection of MEST exposed at the cell surface. In MEST-Myc-DDK transduced cells stained with anti-Myc antibodies in non-permeabilizing conditions most of the cell surface was MEST-negative, but distinct MEST-positive domains were observed (Fig. 6A). At higher magnification they were presented by circular structures with the diameter of 0.3–1.5 μM (Fig. 6B). MEST-positive cell surface domains may represent the sites of fusion of ER-derived vesicles with the plasma membrane. At the same time, applying cell transfection with the MAPPER-GFP construct (kind gift of EJ Dickson, University of California, Davis), which is used to map the bridges between ER and plasma membrane (Chang, Hsieh et al. 2013, Dickson, Jensen et al. 2016), we found distinct localizations of MEST-positive cell surface domains and MAPPER-positive sites (Fig. 6C).

DISCUSSION

Our studies demonstrate the localization of MEST in ER membranes (Fig. 2 and 3) and its absence in the Golgi apparatus (Fig. 4A, B), mitochondria (Fig. 4C, D) and in most of a lipid droplets body and surface except for sites of ER-lipid droplet contact (Fig. 5). ER membrane localization of MEST is also supported by the presence of a long uninterrupted stretch of hydrophobic amino acid residues near its N-terminus (from amino acid 17 to 27), which may represent a potential transmembrane domain. In addition to confirming previous results showing localization of MEST in the membrane component of fractionated mouse adipose tissue (Nikonova, Koza et al. 2008), these studies also begin to define the pattern of ER-localized MEST expression in relation to organelles within an intact cell.

MEST is highly conserved across species and has ~98% identity between the human and mouse proteins at the amino acid level. While its exact function is not yet known, MEST belongs to a large family of α/β hydrolases (Ollis, Cheah et al. 1992, Holmquist 2000) and has homology to epoxide hydrolases which have been shown to catalyze the transformation of epoxy forms of fatty acids to their respective diols (Decker, Arand et al. 2009, El-Sherbeni and El-Kadi 2014). MEST also contains the catalytic triad serine-histidine-aspartate which is associated with serine proteases, lipases and acyltransferases (Carter and Wells 1988, Holmquist 2000). The rapid upregulation of MEST expression after initiation of high fat diet-mediated fat mass expansion in mice (Nikonova, Koza et al. 2008, Voigt, Ribot et al. 2015, Anunciado-Koza, Manuel et al. 2016) and its location within the ER, the established locale of triglyceride production (Suzuki 2017), indicate that MEST may

participate in the metabolism of fatty acids in the process of lipogenesis and simultaneously modulate levels of epoxy- and diol-fatty acid derivatives which are thought to be endogenous mediators of PPARs (Cowart, Wei et al. 2002, Fang, Hu et al. 2006, Spector and Norris 2007). Since multifunctional catalytic activity is common among α/β-hydrolase fold proteins, it is plausible that MEST could have dual function as an epoxide hydrolase as well as a serine protease, lipase or acyltransferase which could be dependent upon the metabolic status of the cell (Cheng, Huang et al. 2012, Marchot and Chatonnet 2012, Lenfant, Hotelier et al. 2013). Recently it has been shown that primary murine-derived mesenchymal progenitor cells from mice with a genetically targeted inactivation of MEST show a greater reduction of adipogenesis after shRNA knockdown of glycerol-3-phosphate acyltransferase 4 (GPAT4) than control cells which suggests that MEST has some endogenous GPAT activity that contributes to triglyceride synthesis and storage. Alternatively, MEST may interact with other protein(s) or via other mechanisms to enhance lipid storage in cells undergoing adipogenesis (Anunciado-Koza, Manuel et al. 2017).

The presence of MEST in the nuclear envelope agrees with the well-established continuity between ER membranes and the exterior nuclear membrane (Selman and Jurand 1964). The exclusion of MEST from mitochondrial and Golgi membranes is interesting because of existence of numerous ER contacts with mitochondria (Rowland and Voeltz 2012) and continuous reversible vesicle-mediated transport between the ER and Golgi (Gomez-Navarro and Miller 2016). Therefore it is likely that this ER preference for MEST is based on specific molecular mechanisms that prevent MEST transport to mitochondrial and Golgi membranes.

Localization of MEST at the lipid droplet-ER contacts reflects the budding of lipid droplets from ER channels (Ben M'barek, Ajjaji et al. 2017). Unlike ER, lipid droplets are covered by phospholipid monolayer, not a bilayer and this feature may prevent the localization of MEST within the lipid droplets envelope. However, localization of MEST at ER-lipid droplet junctions supports the premise that MEST functions to expedite lipid droplet formation in adipocytes undergoing hypertrophy in an obesogenic environment.

Interestingly, MEST demonstrated a distinct spotted localization at the cell surface, and MEST-positive sites were negative for MAPPER-GFP, which is used to identify the ER-PM contacts. This finding indicates that the contacts between ER and PM may vary in their organization and composition.

In conclusion, the demonstration of MEST as an ER-specific protein will facilitate the understanding of its function(s), its role in lipogenesis and the mechanisms of MEST incorporation into the ER membranes.

Supplementary Material

Refer to Web version on PubMed Central for supplementary material.

Acknowledgments

Grant Information:

Grant sponsor: NIH; Grant number: R01DK090361

Grant sponsor: NIGMS; Grant number: P30GM106391

Grant sponsor: NIGMS; Grant number: P30GM103392

The work was supported by NIH grant R01DK090361 (R.A.K.). Support was also provided by the Molecular Phenotyping Core (funded by COBRE; NIGMS P30GM106391) and the Viral Vector and Confocal Imaging Cores (funded by COBRE; NIGMS P30GM103392) at the Maine Medical Center Research Institute. The MAPPER-GFP construct was a kind gift from Eamonn Dickson (University of California, Davis). The authors of this manuscript report no conflicts of interest.

References

Anunciado-Koza RP, Manuel J, Koza RA. Molecular correlates of fat mass expansion in C57BL/6J mice after short-term exposure to dietary fat. Ann N Y Acad Sci. 2016; 1363:50–58. [PubMed: 26647164]

Anunciado-Koza RP, Manuel J, Mynatt RL, Zhang J, Kozak LP, Koza RA. Diet-induced adipose tissue expansion is mitigated in mice with a targeted inactivation of mesoderm specific transcript (Mest). PLoS One. 2017; 12(6):e0179879. [PubMed: 28640866]

Barlowe C. COPII: a membrane coat that forms endoplasmic reticulum-derived vesicles. FEBS Lett. 1995; 369(1):93–96. [PubMed: 7641893]

Ben M'barek K, Ajjaji D, Chorlay A, Vanni S, Foret L, Thiam AR. ER Membrane Phospholipids and Surface Tension Control Cellular Lipid Droplet Formation. Dev Cell. 2017; 41(6):591–604e597. [PubMed: 28579322]

Carter P, Wells JA. Dissecting the catalytic triad of a serine protease. Nature. 1988; 332(6164):564–568. [PubMed: 3282170]

Chang CL, Hsieh TS, Yang TT, Rothberg KG, Azizoglu DB, Volk E, Liao JC, Liou J. Feedback regulation of receptor-induced Ca2+ signaling mediated by E-Syt1 and Nir2 at endoplasmic reticulum-plasma membrane junctions. Cell Rep. 2013; 5(3):813–825. [PubMed: 24183667]

Cheng XY, Huang WJ, Hu SC, Zhang HL, Wang H, Zhang JX, Lin HH, Chen YZ, Zou Q, Ji ZL. A global characterization and identification of multifunctional enzymes. PLoS One. 2012; 7(6):e38979. [PubMed: 22723914]

Cowart LA, Wei S, Hsu MH, Johnson EF, Krishna MU, Falck JR, Capdevila JH. The CYP4A isoforms hydroxylate epoxyeicosatrienoic acids to form high affinity peroxisome proliferator-activated receptor ligands. J Biol Chem. 2002; 277(38):35105–35112. [PubMed: 12124379]

Decker M, Arand M, Cronin A. Mammalian epoxide hydrolases in xenobiotic metabolism and signalling. Arch Toxicol. 2009; 83(4):297–318. [PubMed: 19340413]

Dickson EJ, Jensen JB, Vivas O, Kruse M, Traynor-Kaplan AE, Hille B. Dynamic formation of ER-PM junctions presents a lipid phosphatase to regulate phosphoinositides. J Cell Biol. 2016; 213(1): 33–48. [PubMed: 27044890]

El-Sherbeni AA, El-Kadi AO. The role of epoxide hydrolases in health and disease. Arch Toxicol. 2014; 88(11):2013–2032. [PubMed: 25248500]

Fang X, Hu S, Watanabe T, Weintraub NL, Snyder GD, Yao J, Liu Y, Shyy JY, Hammock BD, Spector AA. Activation of peroxisome proliferator-activated receptor alpha by substituted urea-derived soluble epoxide hydrolase inhibitors. J Pharmacol Exp Ther. 2005; 314(1):260–270. [PubMed: 15798002]

Fang X, Hu S, Xu B, Snyder GD, Harmon S, Yao J, Liu Y, Sangras B, Falck JR, Weintraub NL, Spector AA. 14,15-Dihydroxyeicosatrienoic acid activates peroxisome proliferator-activated receptor-alpha. Am J Physiol Heart Circ Physiol. 2006; 290(1):H55–63. [PubMed: 16113065]

Fujimoto T, Parton RG. Not just fat: the structure and function of the lipid droplet. Cold Spring Harb Perspect Biol. 2011; 3(3)

Gawronska-Kozak B. Preparation and differentiation of mesenchymal stem cells from ears of adult mice. Methods Enzymol. 2014; 538:1–13. [PubMed: 24529430]

Gomez-Navarro N, Miller E. Protein sorting at the ER-Golgi interface. J Cell Biol. 2016; 215(6):769–778. [PubMed: 27903609]

Guo Y, Cordes KR, Farese RV Jr, Walther TC. Lipid droplets at a glance. J Cell Sci. 2009; 122(Pt 6): 749–752. [PubMed: 19261844]

Harris LA, Shew TM, Skinner JR, Wolins NE. A single centrifugation method for isolating fat droplets from cells and tissues. J Lipid Res. 2012; 53(5):1021–1025. [PubMed: 22327205]

Holmquist M. Alpha/Beta-hydrolase fold enzymes: structures, functions and mechanisms. Curr Protein Pept Sci. 2000; 1(2):209–235. [PubMed: 12369917]

Jung H, Lee SK, Jho EH. Mest/Peg1 inhibits Wnt signalling through regulation of LRP6 glycosylation. Biochem J. 2011; 436(2):263–269. [PubMed: 21375506]

Kaneko-Ishino T, Kuroiwa Y, Miyoshi N, Kohda T, Suzuki R, Yokoyama M, Viville S, Barton SC, Ishino F, Surani MA. Peg1/Mest imprinted gene on chromosome 6 identified by cDNA subtraction hybridization. Nat Genet. 1995; 11(1):52–59. [PubMed: 7550314]

Kim DH, Vanella L, Inoue K, Burgess A, Gotlinger K, Manthati VL, Koduru SR, Zeldin DC, Falck JR, Schwartzman ML, Abraham NG. Epoxyeicosatrienoic acid agonist regulates human mesenchymal stem cell-derived adipocytes through activation of HO-1-pAKT signaling and a decrease in PPARgamma. Stem Cells Dev. 2010; 19(12):1863–1873. [PubMed: 20412023]

Koza RA, Nikonova L, Hogan J, Rim JS, Mendoza T, Faulk C, Skaf J, Kozak LP. Changes in gene expression foreshadow diet-induced obesity in genetically identical mice. PLoS Genet. 2006; 2(5):e81. [PubMed: 16733553]

Lenfant N, Hotelier T, Velluet E, Bourne Y, Marchot P, Chatonnet A. ESTHER, the database of the alpha/beta-hydrolase fold superfamily of proteins: tools to explore diversity of functions. Nucleic Acids Res. 2013; 41(Database issue):D423–429. [PubMed: 23193256]

Lewis MJ, Pelham HR. SNARE-mediated retrograde traffic from the Golgi complex to the endoplasmic reticulum. Cell. 1996; 85(2):205–215. [PubMed: 8612273]

Marchot P, Chatonnet A. Enzymatic activity and protein interactions in alpha/beta hydrolase fold proteins: moonlighting versus promiscuity. Protein Pept Lett. 2012; 19(2):132–143. [PubMed: 21933125]

Meijer K, de Vries M, Al-Lahham S, Bruinenberg M, Weening D, Dijkstra M, Kloosterhuis N, van der Leij RJ, van der Want H, Kroesen BJ, Vonk R, Rezaee F. Human primary adipocytes exhibit immune cell function: adipocytes prime inflammation independent of macrophages. PLoS One. 2011; 6(3):e17154. [PubMed: 21448265]

Nikonova L, Koza RA, Mendoza T, Chao PM, Curley JP, Kozak LP. Mesoderm-specific transcript is associated with fat mass expansion in response to a positive energy balance. FASEB J. 2008; 22(11):3925–3937. [PubMed: 18644838]

Ollis DL, Cheah E, Cygler M, Dijkstra B, Frolow F, Franken SM, Harel M, Remington SJ, Silman I, Schrag J, et al. The alpha/beta hydrolase fold. Protein Eng. 1992; 5(3):197–211. [PubMed: 1409539]

Pol A, Gross SP, Parton RG. Review: biogenesis of the multifunctional lipid droplet: lipids, proteins, and sites. J Cell Biol. 2014; 204(5):635–646. [PubMed: 24590170]

Prinz WA. A bridge to understanding lipid droplet growth. Dev Cell. 2013; 24(4):335–336. [PubMed: 23449466]

Rim JS, Mynatt RL, Gawronska-Kozak B. Mesenchymal stem cells from the outer ear: a novel adult stem cell model system for the study of adipogenesis. Faseb J. 2005; 19(9):1205–1207. [PubMed: 15857881]

Rowland AA, Voeltz GK. Endoplasmic reticulum-mitochondria contacts: function of the junction. Nat Rev Mol Cell Biol. 2012; 13(10):607–625. [PubMed: 22992592]

Sanjabi B, Dashty M, Ozcan B, Akbarkhanzadeh V, Rahimi M, Vinciguerra M, van Rooij F, Al-Lahham S, Sheedfar F, van Kooten TG, Spek CA, Rowshani AT, van der Want J, Klaassen R, Sijbrands E, Peppelenbosch MP, Rezaee F. Lipid droplets hypertrophy: a crucial determining factor in insulin regulation by adipocytes. Sci Rep. 2015; 5:8816. [PubMed: 25743104]

Selman GG, Jurand A. An Electron Microscope Study of the Endoplasmic Reticulum in Newt Notochord Cells after Disturbance with Ultrasonic Treatment and Subsequent Regeneration. J Cell Biol. 1964; 20:175–183. [PubMed: 14105208]

Spang A. Retrograde traffic from the Golgi to the endoplasmic reticulum. Cold Spring Harb Perspect Biol. 2013; 5(6)

Spector AA. Arachidonic acid cytochrome P450 epoxygenase pathway. J Lipid Res. 2009; 50(Suppl):S52–56. [PubMed: 18952572]

Spector AA, Norris AW. Action of epoxyeicosatrienoic acids on cellular function. Am J Physiol Cell Physiol. 2007; 292(3):C996–1012. [PubMed: 16987999]

Suzuki M. Regulation of lipid metabolism via a connection between the endoplasmic reticulum and lipid droplets. Anat Sci Int. 2017; 92(1):50–54. [PubMed: 27822589]

Takahashi M, Kamei Y, Ezaki O. Mest/Peg1 imprinted gene enlarges adipocytes and is a marker of adipocyte size. Am J Physiol Endocrinol Metab. 2005; 288(1):E117–124. [PubMed: 15353408]

Voigt A, Ribot J, Sabater AG, Palou A, Bonet ML, Klaus S. Identification of Mest/Peg1 gene expression as a predictive biomarker of adipose tissue expansion sensitive to dietary anti-obesity interventions. Genes Nutr. 2015; 10(5):477.

Waldman M, Bellner L, Vanella L, Schragenheim J, Sodhi K, Singh SP, Lin D, Lakhkar A, Li J, Hochhauser E, Arad M, Darzynkiewicz Z, Kappas A, Abraham NG. Epoxyeicosatrienoic Acids Regulate Adipocyte Differentiation of Mouse 3T3 Cells, Via PGC-1alpha Activation, Which Is Required for HO-1 Expression and Increased Mitochondrial Function. Stem Cells Dev. 2016; 25(14):1084–1094. [PubMed: 27224420]

Watson P, Stephens DJ. ER-to-Golgi transport: form and formation of vesicular and tubular carriers. Biochim Biophys Acta. 2005; 1744(3):304–315. [PubMed: 15979504]

Wilfling F, Wang H, Haas JT, Krahmer N, Gould TJ, Uchida A, Cheng JX, Graham M, Christiano R, Frohlich F, Liu X, Buhman KK, Coleman RA, Bewersdorf J, Farese RV Jr, Walther TC. Triacylglycerol synthesis enzymes mediate lipid droplet growth by relocalizing from the ER to lipid droplets. Dev Cell. 2013; 24(4):384–399. [PubMed: 23415954]

Zha W, Edin ML, Vendrov KC, Schuck RN, Lih FB, Jat JL, Bradbury JA, DeGraff LM, Hua K, Tomer KB, Falck JR, Zeldin DC, Lee CR. Functional characterization of cytochrome P450-derived epoxyeicosatrienoic acids in adipogenesis and obesity. J Lipid Res. 2014; 55(10):2124–2136. [PubMed: 25114171]

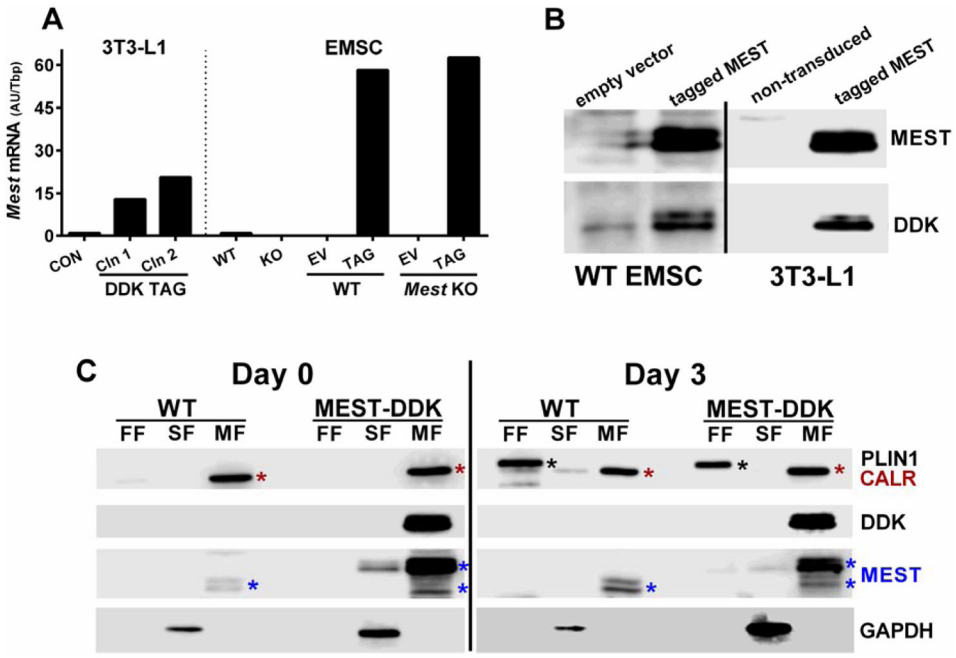

Figure 1.

Myc-DDK tagged MEST in membrane fraction of fractionated cells. (A) MEST mRNA expression measured by qRT-PCR in two clones (Cln) of 3T3-L1 preadipocytes and EMSC cell lines derived from wildtype (WT) and *Mest* knockout (KO) mice after integration of an empty lentiviral vector (EV) or lentiviral vector expressing recombinant Myc-DDK tagged *Mest*. (B) Western blot analyses of MEST and DDK in WT EMSC and 3T3-L1 preadipocytes that are transduced with EV, non-transduced, or transduced with a lentiviral vector expressing recombinant Myc-DDK tagged *Mest*. (C) Fractionation of WT EMSC and EMSC with lentiviral-expressed Myc-DDK tagged MEST (MEST-DDK) prior to and after 3 days of adipogenic differentiation shows that expression of endogenous and tagged MEST (DDK) are co-fractionated with the ER protein calreticulin (CALR) predominantly in the membrane fraction (MF). Very little endogenous or tagged MEST co-localizes with GAPDH in the soluble fraction (SF) or with perilipin (PLIN1) and lipid droplets in floating fraction (FF).

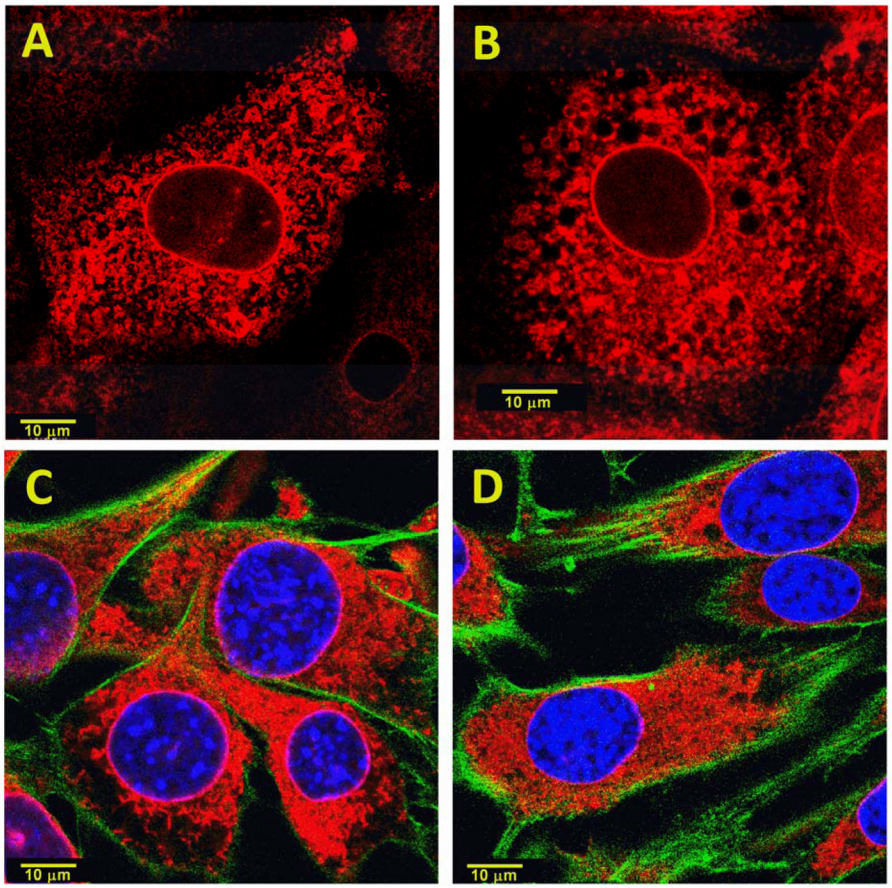

Figure 2.

Reticular pattern of MEST (red) distribution in the cytoplasm of a MEST-Myc transduced 3T3-L1 cell (A) and a differentiated wildtype EMSC cell (B). Panel C and D shows filamentous actin (stained with Alexa-488 conjugated phalloidin; green) and nuclei (blue) in undifferentiated EMSC from wildtype (C) and *Mest* KO (D) mice.

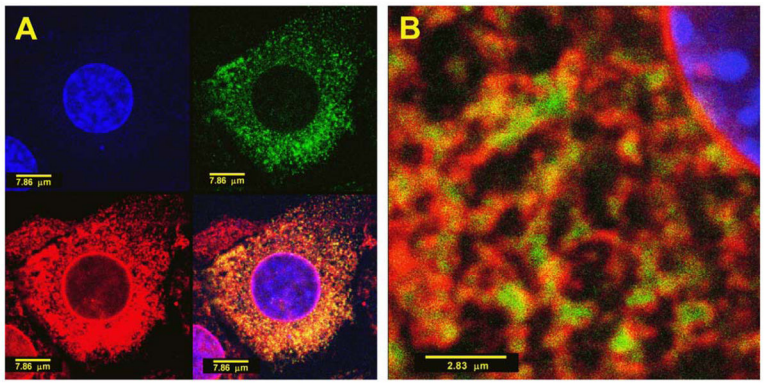

Figure 3.

MEST and endoplasmic reticulum. EMSC (A) and 3T3-L1 cells (B) were co-stained for MEST (anti-Myc antibodies, red), ER (anti-PDI antibodies, green) and DNA (Hoechst, blue). MEST and the ER marker PDI are co-localized (A), and higher magnification (B) shows the localization of PDI inside the MEST-positive structures.

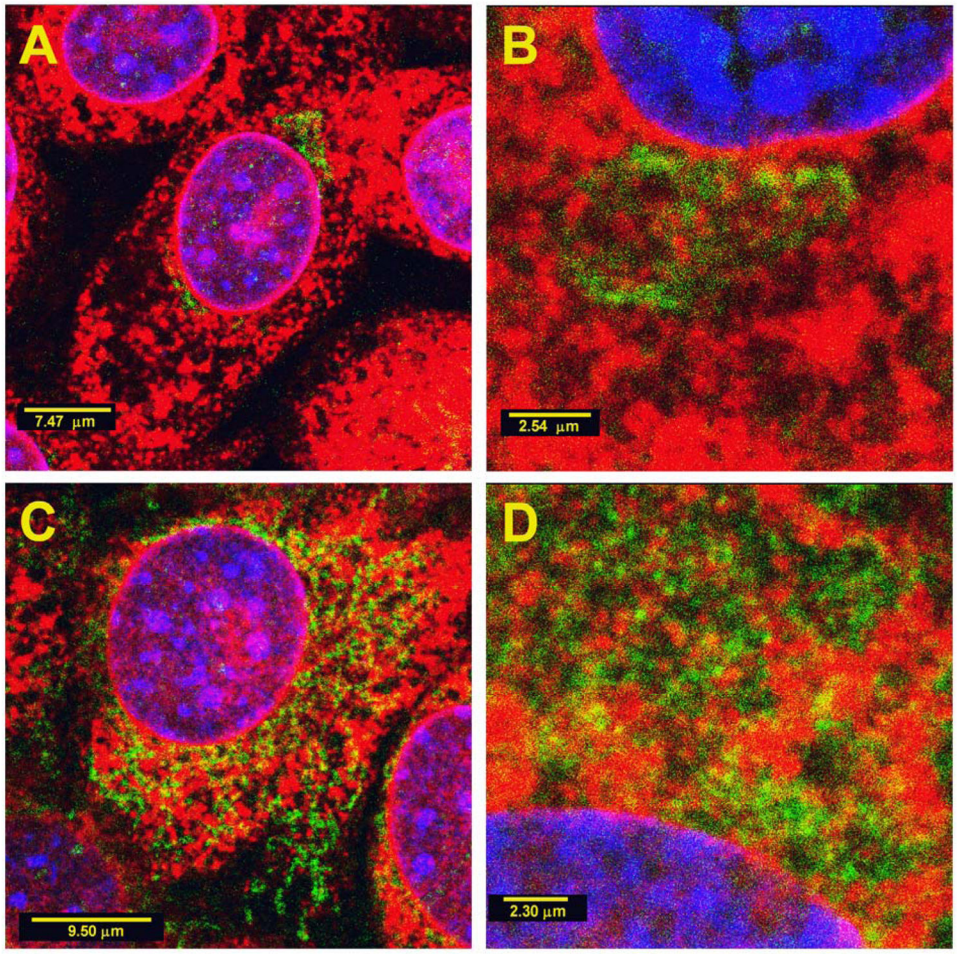

Figure 4.

MEST, Golgi and mitochondria. EMSC (A) and 3T3-L1 cells (B) were co-stained for MEST (anti-Myc antibodies, red), Golgi (anti-GM130 antibodies, green) and DNA (Hoechst, blue). MEST and Golgi show distinct localization that is especially evident at higher magnification (B). EMSC (C) and 3T3-L1 cells (D) were co-stained for MEST (anti-Myc antibodies, red), mitochondria (anti-hexokinase antibodies, green) and DNA (Hoechst, blue). The higher magnification images (B and D) were taken from different cells than those with lower magnification (A and C). Mitochondria and ER are distinctly localized, although they often contact.

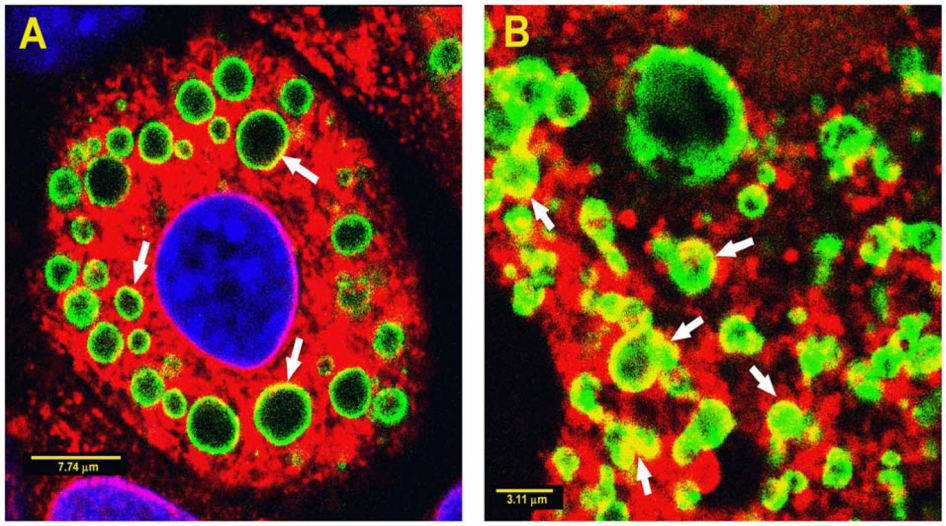

Figure 5.

MEST and lipid droplets. Differentiated EMSC (A) and 3T3-L1 cells; at higher magnification (B), were co-stained for MEST (anti-Myc antibodies, red), lipid droplets (anti-perilipin antibodies, green) and DNA (Hoechst, blue). MEST-positive structures and lipid droplets are distinctly localized, although they exhibit frequent contacts as indicated by arrows.

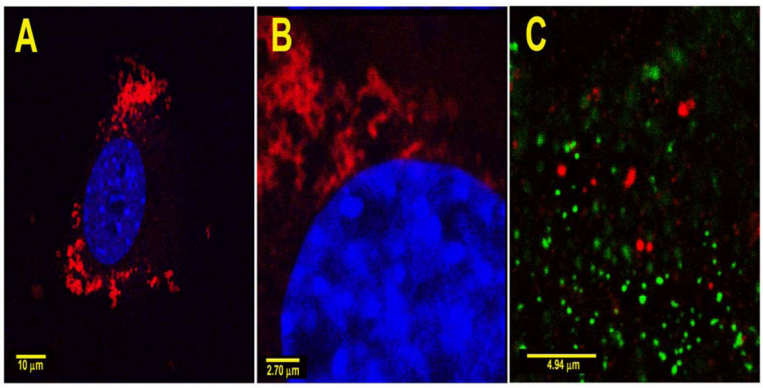

Figure 6.

Cell surface exposure of MEST. (A) Formalin fixed non-permeabilized EMSC were stained for MEST (anti-Myc antibodies, red) and DNA (Hoechst, blue). Circular MEST positive structures (B) are exposed at the cell surface. (C) Formalin fixed non-permeabilized 3T3-L1 cells stably transduced with MEST-Myc and transiently co-transfected with MAPPER-GFP were stained for MEST (anti-Myc antibodies, red) to show cell surface exposure of MEST and MAPPER-GFP. MEST positive structures exposed at the cell surface are localized distinctly from MAPPER-positive domains.